

# Convective magneto-rotational instabilities in accretion disks

E. van der Swaluw<sup>1</sup>, J. W. S. Blokland<sup>1,2</sup>, and R. Keppens<sup>1,2</sup>

<sup>1</sup> FOM-Institute for Plasma Physics Rijnhuizen, P.O. Box 1207, 3430 BE Nieuwegein, The Netherlands

<sup>2</sup> Association EURATOM-FOM, Trilateral Euregio Cluster

**Abstract.** We present a study of instabilities occurring in thick magnetized accretion disks. We calculate the growth rates of these instabilities and characterise precisely the contribution of the magneto-rotational and the convective mechanism. All our calculations are performed in radially stratified disks in the cylindrical limit. The numerical calculations are performed using the appropriate local dispersion equation solver discussed in Blokland et al. (2005). A comparison with recent results by Narayan et al. (2002) shows excellent agreement with their approximate growth rates only if the disks are weakly magnetized. However, for disks close to equipartition, the dispersion equation from Narayan et al. (2002) loses its validity. Our calculations allow for a quantitative determination of the increase of the growth rate due to the magneto-rotational mechanism. We find that the increase of the growth rate for long wavelength convective modes caused by this mechanism is almost negligible. On the other hand, the growth rate of short wavelength instabilities can be significantly increased by this mechanism, reaching values up to 60%.

**Key words.** Accretion Disks – instabilities – stars:accretion – magnetohydrodynamics

## 1. Introduction

Accretion disks are present around a variety of astrophysical objects, ranging from young proto-stars in star formation regions to massive black holes in the centers of galaxies. A standard model of a geometrically thin accretion disk was introduced in the early seventies by Shakura & Sunyaev (1973). In their model angular momentum is transported outwards by an anomalous viscosity mechanism, which is parametrised by the  $\alpha$ -parameter. This parameter scales linearly with the radial-azimuthal component of the stress tensor, which is associated with the viscous torque providing the angular momentum transport. The assumption of a geometrically thin disk implies that the gravitational energy release by viscous dissipation is locally radiated away.

It was realised in the early nineties that the anomalous viscosity mechanism can be provided by the turbulence arising from the magneto-rotational instability (Balbus & Hawley 1991). These authors showed that this essentially magnetic instability is a very robust one, occurring in weakly magnetized thin accretion disks.

However, in recent years, Chandra observations have found examples of underluminous black holes at X-ray frequencies. A good example is our own Galactic Center, Sgr A\* (Baganoff et al. 2001), and the galactic center of the elliptic galaxy M87 (Di Matteo et al. 2003). These obser-

vations might be explained in the context of nonradiating accretion flows, which are still using the  $\alpha$  description from Shakura & Sunyaev (1973), but are no longer geometrically thin (Narayan & Li 1994). One of these models which has gained a lot of interest in the literature in recent years is the convection-dominated accretion flow (CDAF). In these type of accretion flow models, the transport of the angular momentum outwards by the turbulence arising from the magneto-rotational instability is partly counterbalanced by transport inwards due to convective motion occurring in these *thick* accretion disks. Therefore the accretion rate might be efficiently reduced, which might explain the lower observed X-ray luminosities in Sgr A\* and the central region of M87.

Recent studies of these CDAF-type of disks, in which both convective and magneto-rotational instabilities can be found, have been performed by Balbus & Hawley (2002) and Narayan et al. (2002). These authors have used a linear stability analysis and identified unstable long-wavelength modes with a convective nature, and short-wavelength modes with a more dominant MRI behaviour.

In this paper, we will elaborate on the work from Narayan et al. (2002). These authors have considered a differentially rotating and thermally stratified plasma, with a weak axial magnetic field. They use the equation for the growth rate as obtained by Balbus & Hawley (1991), who used linear stability theory to derive the latter. Narayan et al. (2002) consider five models of an accretion disk, each of these five models has a different value of the assumed uni-

---

Send offprint requests to: E. van der Swaluw, e-mail: swaluw@rijnh.nl

form Brunt-Väisälä frequency. Their results clearly show the rise of a plateau in the obtained growth rate at low axial wavenumbers as the Brunt-Väisälä frequency is increased. They argue that the modes in this plateau are identified as convective modes, once the Brunt-Väisälä frequency exceeds the epicyclic frequency, i.e. the Høiland criterion (Tassoul, 1987). The exact nature of a mode in this plateau is identified using results from the linear stability theory as performed by Balbus & Hawley (1991, 2002).

We follow up on the above mentioned work, but we will numerically solve a sixth order polynomial dispersion relation, using the Local Dispersion Equation Solver (LODES), which was already discussed in Blokland et al. (2005). We will not only consider weakly magnetized disks, but also consider models which are closer to equipartition. We will consider a differentially rotating plasma for which the equilibrium quantities are power-law profiles of the radius. Furthermore, we explicitly define a value for the scale height of the disk  $H$  with respect to the radius  $r$ , with the free parameter  $\epsilon = H/r$ .

In our present analysis we only consider axisymmetric perturbations, which means that in a model with a purely toroidal magnetic field, the magneto-rotational mechanism is excluded. Therefore in such models, the obtained modes are purely convective. The growth rates from these modes can be compared to a similar model which includes a *weak* axial magnetic field. This enables one to observe the increase of the growth rate due to the presence of the magneto-rotational mechanism.

This paper is organised as follows: in section 2 we discuss our model, section 3 shortly recalls the model from Narayan et al. (2002), in section 4 we present our results, including a comparison with the results from Narayan et al. (2002), finally in section 5 we present our conclusions.

## 2. Accretion disk model

### 2.1. Equilibrium of a differentially rotating plasma

We want to investigate the growth rate of instabilities occurring in a magnetized accretion disk. In order to quantify instabilities using a linear analysis, one has to consider an MHD equilibrium. In our case, this equilibrium is one of a differentially rotating plasma, which is radially stratified. In our model the density, pressure, magnetic field strength and toroidal velocity only depend on the radius  $r$ . This type of model is sometimes referred to as an accretion disk in the cylindrical limit (see for example Hawley 2001).

We use an equilibrium as in Blokland et al. (2005), generalised with an additional parameter  $a$ , which is introduced in order to allow for convective instabilities. The following profiles are used for respectively density  $\rho$ , thermal pressure  $p$ , toroidal magnetic field  $B_\theta$ , axial magnetic

field  $B_z$  and the toroidal velocity  $v_\theta$ :

$$\rho = r^{-(3+a)/2}, \quad (1)$$

$$p = \epsilon^2 r^{-(5+a)/2}, \quad (2)$$

$$B_\theta = -\alpha_1 \sqrt{\frac{2\epsilon^2}{\beta(\alpha_1^2 + \alpha_2^2)}} r^{-(5+a)/4}, \quad (3)$$

$$B_z = \alpha_2 \sqrt{\frac{2\epsilon^2}{\beta(\alpha_1^2 + \alpha_2^2)}} r^{-(5+a)/4}, \quad (4)$$

$$v_\theta = V_0 r^{-1/2}, \quad (5)$$

$$(6)$$

in which the  $\alpha$ -parameters can be expressed as the ratio of both the toroidal and axial magnetic field over the total magnetic field  $B$  like:

$$B_\theta/B = -\alpha_1/\sqrt{\alpha_1^2 + \alpha_2^2}, \quad (7)$$

$$B_z/B = \alpha_2/\sqrt{\alpha_1^2 + \alpha_2^2}, \quad (8)$$

and the parameter  $V_0$  is defined as:

$$V_0^2 = GM_* - \frac{\epsilon^2}{2\beta(\alpha_1^2 + \alpha_2^2)} ((5+a)(1+\beta)(\alpha_1^2 + \alpha_2^2) - 4\alpha_1^2). \quad (9)$$

Here,  $G$  and  $M_*$  denote respectively the gravitational constant and the mass of the central object. Finally, the parameter  $\beta$  denotes the radially constant ratio between the thermal pressure and the total magnetic pressure  $B^2/2$ , i.e.  $\beta \equiv 2p/B^2$ .

The above power-law profiles satisfy the radial force balance equation in cylindrical coordinates:

$$[p + \frac{1}{2}B^2]' + \frac{B_\theta^2}{r} = \frac{\rho v_\theta^2}{r} - \rho g, \quad (10)$$

here  $g$  denotes  $GM_*/r^2$ , and the prime indicates the derivative with respect to the radius  $r$ .

The differences between our equilibrium and the one from Narayan et al. (2002) are: 1) we *explicitly* define the above mentioned equilibrium quantities by using power-law profiles as a function of radius  $r$ ; 2) we include the toroidal magnetic field component  $B_\theta$ ; 3) we define a ratio of the scale height  $H$  over the radius  $r$ , i.e.  $\epsilon \equiv H/r$ , in order to quantify the thickness of our disk model; and 4) we do not exclude disks close to equipartition ( $\beta$  is a free parameter).

### 2.2. Determining the growth rate of instabilities

We use the local dispersion equation solver (LODES), which was recently discussed by Blokland et al. (2005). This code calculates the growth rate of the most unstable mode in a given MHD equilibrium for a given radial ‘wavenumber’ ( $q$ ), and a toroidal ( $m$ ) and axial wavenumber ( $k$ ) at a given position  $r_1$ . We will only consider axisymmetric perturbations ( $m = 0$ ) in this paper.

In order to determine the radial ‘wavenumber’  $q$ , we use the method as discussed by Blokland et al. (2005). It

was shown there that under certain assumptions, the numerical solution of the full set of linearised compressible MHD equations governing all MHD modes in disk equilibria obeying Eq. (10), can be avoided for modes obeying a local dispersion equation found from WKB analysis. Excellent agreement between the growth rate and the eigenfunction behaviour was demonstrated when position  $r_i$  and associated ‘wavenumber’  $q$  were properly calculated from the full numerical solution. In this paper we follow Balbus & Hawley (1991) and Narayan et al. (2002), who effectively take  $q = 0$ , in order to make a direct comparison with their calculations. We notice that we only observed a difference of the order of 1% in our obtained growth rates, with respect to our calculations for which the ‘wavenumber’  $q$  was properly calculated.

The local dispersion equation solver finds the root of a sixth order polynomial, using Laguerre’s method (Press et al. 1988). This sixth order polynomial dispersion equation represents the local dispersion equation as an approximation to the true 10<sup>th</sup> degree WKB local dispersion equation (Blokland et al., 2005), which is more general than the one discussed by Narayan et al. (2002): 1) it allows to calculate the growth rate of instabilities for an equilibrium which has both an axial and a toroidal magnetic field component; and 2) the equilibrium can be either weakly magnetized, or close to equipartition. Narayan et al. (2002) could not consider disks close to equipartition, because the fourth order polynomial from Balbus & Hawley (1991) was derived *assuming* a weak axial and no toroidal magnetic field component.

### 3. Accretion disks with convection

#### 3.1. A thick accretion disk

One of the key parameters of our MHD equilibrium is the parameter  $\epsilon$ , which is taken as a constant free parameter. This parameter was introduced by Shakura & Sunyaev (1973) in their model of geometrically thin accretion disks, which are Keplerian rotating. The physical interpretation of  $\epsilon$  in these models is the same as in the MHD equilibrium we consider here, i.e.  $\epsilon = c_s/v_\theta \simeq H/r$ , where  $c_s$  denotes the sound speed. MRI instabilities in thin accretion disk models were considered by Blokland et al. (2005). However, in this paper we consider values of  $\epsilon \sim 1$ , i.e. we are in the regime of sub-Keplerian rotating disks (see e.g. Narayan & Yi 1994). For these cases we stick to the interpretation  $\epsilon \simeq H/r$ , noting that the identification  $\epsilon = c_s/v_\theta$  is not valid anymore. Typically,  $c_s/v_\theta$  in our models will be larger up to a maximum factor of order  $\sim 10$ . As mentioned in section 2, our MHD equilibrium is an example of an accretion disk model in the cylindrical limit. One has to realise that results from these type of models approximate the *interior* of a real height-dependent accretion disk. This approximation is correct as long as the axial wavenumber  $k$  is much larger than the inverse of the scale height  $H$ . Therefore the identity  $k \gg 2\pi/(\epsilon r)$  has to be satisfied in

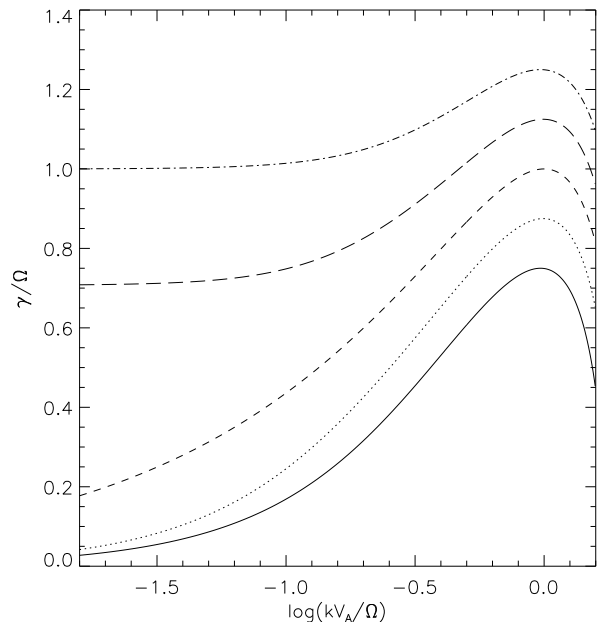


**Fig. 1.** Dimensionless growth rate  $\gamma/\Omega$  as a function of dimensionless wavevector  $kv_A/\Omega$  for accretion disk models from Narayan et al. (2002). The five growth rates shown are from five different solutions:  $N^2/\Omega^2 = 0.0$  (solid line);  $N^2/\Omega^2 = 0.5$  (dotted line);  $N^2/\Omega^2 = 1.0$  (short-dashed line);  $N^2/\Omega^2 = 1.5$  (long-dashed line);  $N^2/\Omega^2 = 2.0$  (dot-dashed line).

our calculations in order to connect these results with the interior of an accretion disk.

#### 3.2. Convective instabilities

As discussed in section 2, Narayan et al. (2002) also considered an equilibrium of a differentially rotating plasma, which only allows for a weak axial magnetic field component. Furthermore, their equilibrium quantities depend on radius  $r$ , but are not explicitly defined as power-laws obeying the radial force balance equation (10). Therefore, in order to introduce convective instabilities in their model, they describe the stratification of the differentially rotating plasma in terms of a free parameter  $N^2$ , which is directly related to the Brunt-Väisälä frequency  $N_{\text{BV}}$ :

$$N^2 = -N_{\text{BV}}^2 = \frac{3}{5\rho} \frac{dp}{dr} \frac{d \ln(p\rho^{-5/3})}{dr}. \quad (11)$$

In a weakly-magnetized rotating medium, the onset of convection is determined by the Høiland criterium, i.e.  $N^2 > \kappa^2 (\equiv 2v_\theta(rv_\theta)'/r^2)$ , where  $\kappa$  is the epicyclic frequency. Furthermore, they assume a purely Keplerian system, which means that  $\kappa^2 = \Omega_K^2$ , therefore convective instabilities will be present in their model when  $N^2 > \Omega^2$ . Narayan et al. (2002) present growth rates of instabilities as a function of the axial wavenumber. They use the equation for the growth rate as derived by Balbus & Hawley (1991). They normalise their obtained growth rates to the

rotational frequency, furthermore the wavevector is multiplied by the Alfvén velocity  $V_A$ , and also normalised to the rotational frequency. In this way the only free parameter left for the growth rate profiles is the parameter  $N^2/\Omega^2$ . Figure 1 is showing these scaled growth rates for the different values of  $N^2/\Omega^2$  as considered by Narayan et al. (2002).

In our cylindrical accretion disk model with power-law equilibrium profiles one can calculate  $N^2/\Omega^2$ , and make a direct comparison with the work of Narayan et al. (2002). Furthermore, it can be shown that in our MHD equilibrium the equality  $\kappa^2 = \Omega^2$  is always valid, even if the system is not Keplerian rotating (i.e. when  $\epsilon \sim 1$ ). Therefore our MHD equilibrium will also be convectively unstable once  $N^2 > \Omega^2$ , like in the model from Narayan et al. (2002), the difference being that our models captures significant deviations from *Keplerian rotating* disks by means of the  $\epsilon$  parameter ( $\Omega^2 \neq \Omega_K^2$ ).

The Høiland criterium is valid for a hydrodynamical equilibrium, but strictly speaking it is not valid for an MHD equilibrium which is weakly magnetized. However, it can be used as an indication for convective instabilities at those wavenumbers where the restoring magnetic tension force is much smaller than the buoyancy force (see also Christodoulou et al., 2003). These last authors derived a stability criterium for axial perturbations for magnetized equilibria with purely toroidal magnetic fields. This criterium is valid for all values of the plasma parameter  $\beta$ , which therefore includes equilibria which are weakly magnetized or close to equipartition. Therefore this criterium could be used to determine the presence of convective instabilities in our models with purely toroidal magnetic fields. The criterium can also be derived from the local dispersion equation (see e.g. Keppens et al. (2002); Blokland et al. (2005); Wang et al. (2004)).

### 3.3. A model for the interior of a thick accretion disk

In our MHD equilibrium, the parameter  $\epsilon$  is a free parameter to be interpreted as related to the scale-height  $H$  at each radial position  $r$ . In order to perform a meaningful stability calculation for an accretion disk, the wavenumbers of the unstable modes considered must be such that they are able to manifest themselves in the *interior* of the accretion disk. These instabilities *fit* into the interior of the considered accretion disk model once the corresponding axial wavenumber  $k > k_{\min} \equiv 2\pi/H$ . The analysis from Narayan et al. (2002) shows a maximum of the growth rate at  $\log(kV_A/\Omega) \sim 0.0$  (see Figure 1). We therefore choose our MHD equilibria such that the numerical value of  $\log(k_{\min}V_A/\Omega)$  is typically less than  $\sim -1.5$ . For these models, all unstable modes found with an axial wavenumber  $k > k_{\min}$  *fit* into the interior of the considered disk model, and include the most unstable ones.

We found that in order to satisfy the restriction  $k > k_{\min}$  with  $\log(k_{\min}V_A/\Omega) \sim -1.5$  a high ratio of the toroidal magnetic field strength to the axial magnetic

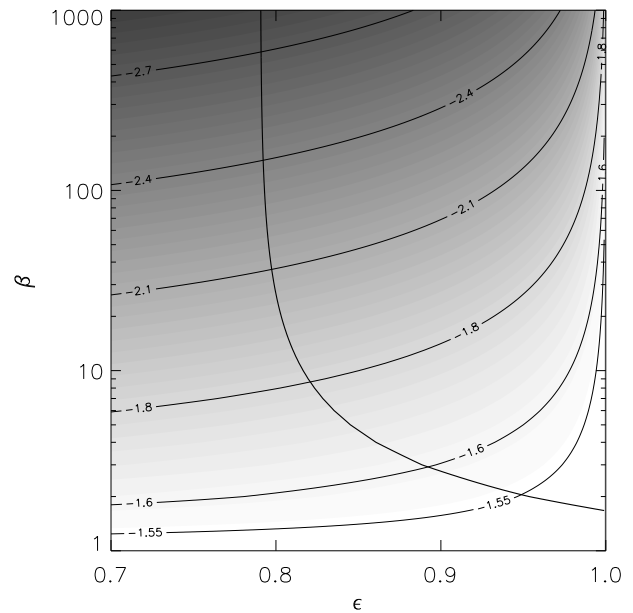


**Fig. 2.** Logarithmic gray-scale plot of the value  $\log(k_{\min}V_A/\Omega)$  in the model for which  $\alpha_1 = 300.0, \alpha_2 = 1.0$  and  $a = -3.0$ . The solid thick line corresponds with  $N^2 = \Omega^2$ . The thick solid curve for the Høiland criterium deviates from a straight vertical line, because of the *dynamical importance* of the magnetic field on the equilibrium for low values of  $\beta$ .

field strength is needed. Figure 2 shows the parameter  $\log(k_{\min}V_A/\Omega)$  as a function of the parameters  $\epsilon$  and  $\beta$  of our model, for which the other parameters have been fixed. Indeed for most values of  $\epsilon$  and  $\beta$  the corresponding numerical value  $\log(k_{\min}V_A/\Omega) < -1.5$ . The thick solid line in Figure 2 marks the Høiland criterium, i.e.  $N^2 = \Omega^2$ . The models on the right hand side of this line are convectively unstable, the models on the left hand side are convectively stable. Notice that the line  $N^2 = \Omega^2$  can be drawn uniquely as a function of  $\beta$  and  $\epsilon$  once  $\alpha_1$  and  $\alpha_2$  are determined. This is because the numerical value of  $N^2/\Omega^2$ , calculated from the equilibrium presented in section 2, does not depend on the radius  $r$ .

As argued above we will choose a configuration of an accretion disk with most of the magnetic field strength in the toroidal component, in order to allow for both convective and magneto-rotational instabilities. The values of the ratio of the Brunt-Väisälä frequency and the rotational frequency marks the free parameter in the paper from Narayan et al.(2002). We plot the numerical value of this parameter in our models in figure 3. We have plotted contours with  $N^2/\Omega^2 = 0.5, 1.0, 1.5, 2.0$ , corresponding to the models discussed in Narayan et al.(2002). It can be noted that in very weakly magnetized, thick disk models we obtain high values for  $N^2/\Omega^2$ , the highest value being  $N^2/\Omega^2 = 600$  (model A in Table 1). Those are expected to be rigorously convective in a pure hydrodynamical sense.

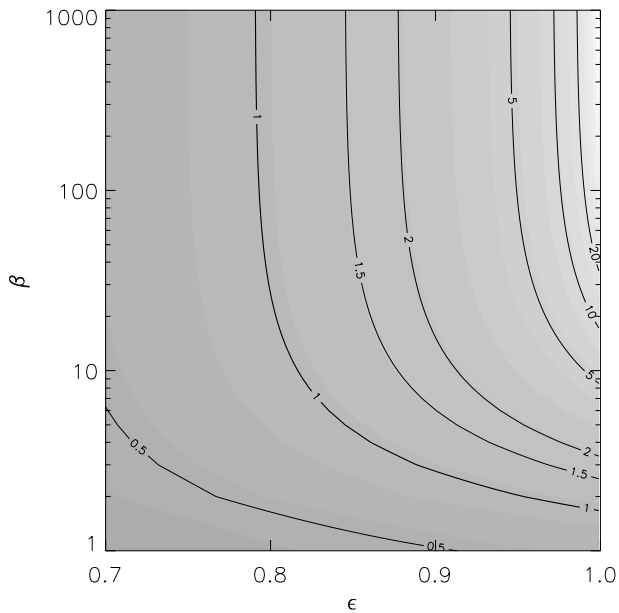


**Fig. 3.** Gray-scale plot of the parameter  $N^2/\Omega^2$  in the model for which  $\alpha_1 = 300.0$ ,  $\alpha_2 = 1.0$  and  $a = -3.0$ .

## 4. Accretion disks with two instabilities

### 4.1. Introduction

We present the results from a linear analysis performed for different MHD equilibria, using the local dispersion equation solver (LODES). In our calculations we will only consider equilibria with a constant density ( $a = -3.0$ ), while most of the magnetic field strength is in the toroidal direction ( $\alpha_1 = 300.0$ ;  $\alpha_2 = 1.0$ ). Finally, we will only consider thick accretion disk models by considering MHD equilibria with  $\epsilon \geq 0.8$ , in order to allow for mixed convective magneto-rotational instabilities. We will consider five different MHD equilibria and calculate the growth rates of the unstable modes. Additionally, we will repeat these calculations for all five models with the only difference that the axial magnetic field equals zero ( $\alpha_2 = 0.0$ ). Since we are only considering axisymmetric perturbations, these last calculations yield instabilities which can not have a magneto-rotational nature, and are purely convective instabilities. Because the axial magnetic fields are weak, comparing the growth rates of a model with or without the axial magnetic field component provides a quantitative measure of the magneto-rotational contribution of an unstable mode in the interior of an accretion disk.

### 4.2. Weakly magnetized disks: from sub-Keplerian to near-Keplerian disks

In this subsection, we will investigate the influence of the parameter  $\epsilon$  on the nature of the instabilities in weakly magnetized ( $\beta = 1000$ ) MHD equilibria (models A-D, Table 1). We will present the growth rates of the instabil-

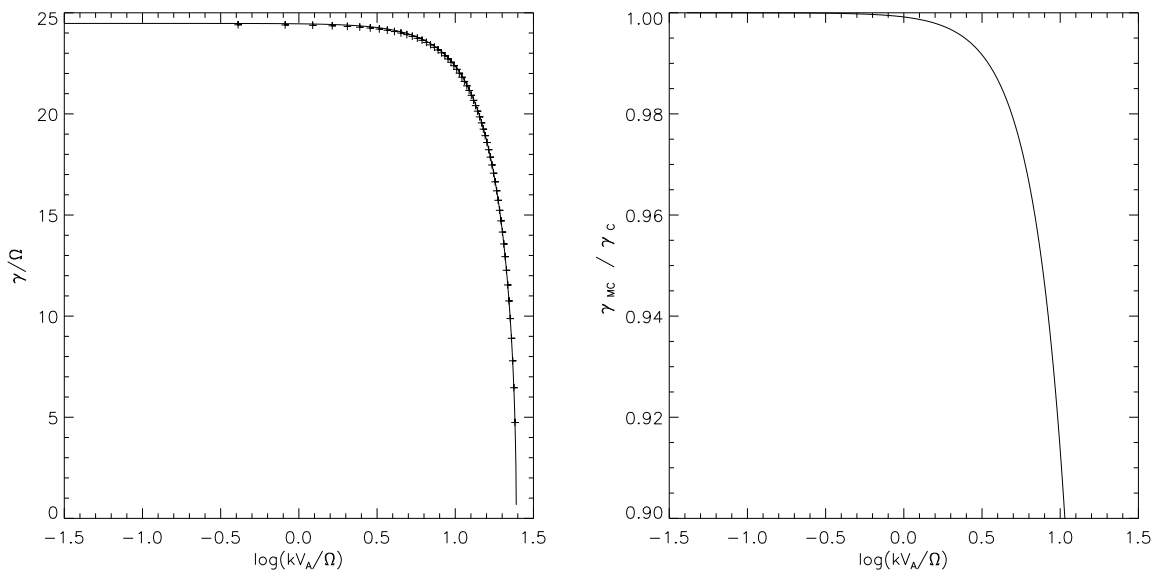
Sim	$\epsilon$	$\beta$	$N^2/\Omega^2$
A	1.0	1000.0	600.0
B	0.94	1000.0	4.5
C	0.88	1000.0	2.0
D	0.845	1000.0	1.5
E	1.0	20.0	12.0
F	1.0	10.0	6.0

**Table 1.** Parameters of accretion disk models: all the models considered have  $\alpha_1 = 300$ ,  $a = -3$  and  $\alpha_2 = 1$  ( $\alpha_2 = 0$ ) for models with (without) axial magnetic field.

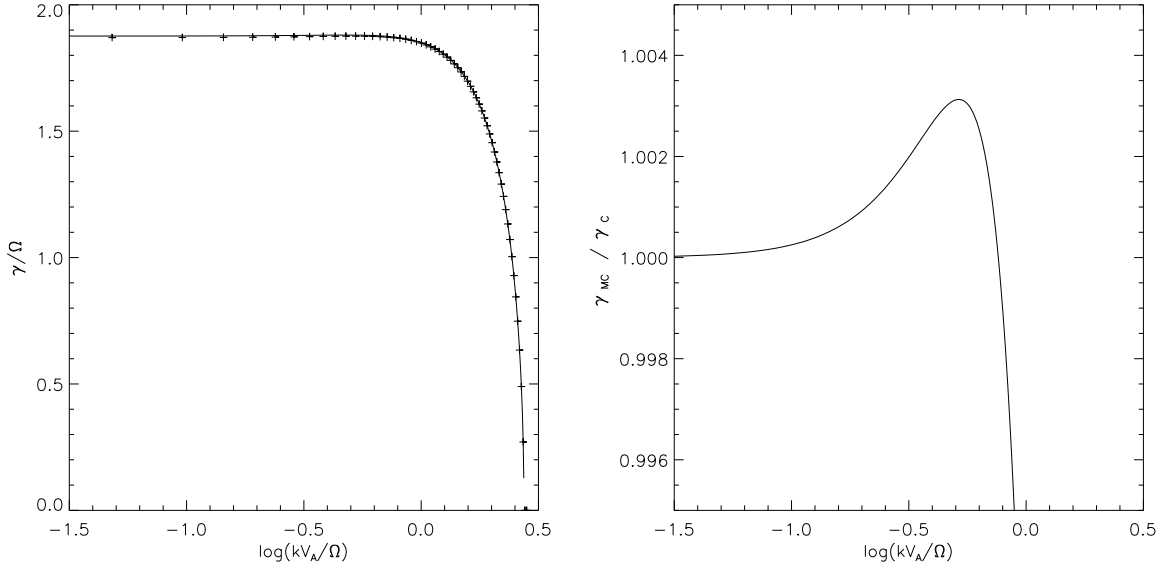
ities in our model as a function of the axial wavenumber, using the same scaling as Narayan et al. (2002).

Figure 4 shows our results for model A, which has a corresponding value of the ratio  $N^2/\Omega^2 = 600$  (model A, Table 1). The left panel shows a comparison between our calculations for the growth rate of the instabilities (crosses) and the calculation from Narayan et al. (2002) (solid line). There is perfect agreement between both results. The right panel shows the ratio of the growth rate of model A with an axial magnetic field ( $\alpha_2 = 1.0$ ) with respect to model A without an axial magnetic field ( $\alpha_2 = 0.0$ ). The model without axial magnetic field excludes the magneto-rotational mechanism completely. One can see that the ratio never exceeds unity, implying that there is no enhancement of the growth rate due to the magneto-rotational mechanism. Furthermore, we observe in the left and right panel that there is no observed maximum value of the growth rate at  $\log(kv_A/\Omega) \approx 0.0$ , a feature also associated with the magneto-rotational instability. Therefore, the observed instabilities have a (nearly) completely convective nature in this particular disk model, as expected from the very high value of  $N^2/\Omega^2$ .

Figure 5 shows our results for model B, which has a corresponding value of the ratio  $N^2/\Omega^2 = 4.5$  (model B, Table 1). One can see in the left panel that the growth rate from our calculations (crosses) again matches the solution for the growth rate (solid line) from Narayan et al. (2002), despite the fact that we consider an overall weak, but predominantly toroidal magnetic field. The right panel of figure 5 shows the ratio of the growth rate of model B with axial magnetic field ( $\alpha_2 = 1.0$ ), with respect to model B without an axial magnetic field component ( $\alpha_2 = 0.0$ ). It is observed that there is an overall small contribution (less than 1 percent) to the growth rates by the magneto-rotational mechanism. This indicates that the unstable



**Fig. 4.** Left panel: dimensionless growth rate  $\gamma/\Omega$  as a function of dimensionless wavenumber  $kv_A/\Omega$  for MHD equilibrium A (see table 1). The solid line corresponds with the solution from Narayan et al. (1994). The crosses correspond to the solution using the code LODES. Right panel: ratio of the growth rate  $\gamma_{MC}$  with ( $\alpha_2 = 1.0$ ) and the growth rate  $\gamma_C$  without ( $\alpha_2 = 0.0$ ) an axial magnetic field component as a function of the dimensionless wavenumber  $kv_A/\Omega$ .



**Fig. 5.** Left panel: dimensionless growth rate  $\gamma/\Omega$  as a function of dimensionless wavenumber  $kv_A/\Omega$  for MHD equilibrium B (see table 1). The solid line corresponds with the solution from Narayan et al. (1994). The crosses correspond to the solution using the code LODES. Right panel: ratio of the growth rate  $\gamma_{MC}$  with ( $\alpha_2 = 1.0$ ) and the growth rate  $\gamma_C$  without ( $\alpha_2 = 0.0$ ) an axial magnetic field component as a function of the dimensionless wavenumber  $kv_A/\Omega$ .

modes have a dominant convective nature in this model, like in model A.

In model C, the thickness of the disk model has been reduced further, such that the obtained ratio  $N^2/\Omega^2 \simeq 2.0$  equals the maximum value Narayan et al. (2002) have considered in their paper. The left panel of Figure 6 shows the calculated growth rates (crosses) of this MHD equilibrium, and there is a perfect match with the solution (solid line)

from Narayan et al.(2002). The right panel of Figure 6 shows the ratio of the growth rate of model C with axial magnetic field ( $\alpha_2 = 1.0$ ) with respect to model C without an axial magnetic field component ( $\alpha_2 = 0.0$ ). The contribution from the magneto-rotational mechanism is significant, of order 25 percent around values of the wavenumber where the growth rate has its maximum: this increase indicates that the unstable modes in this range of wavenum-

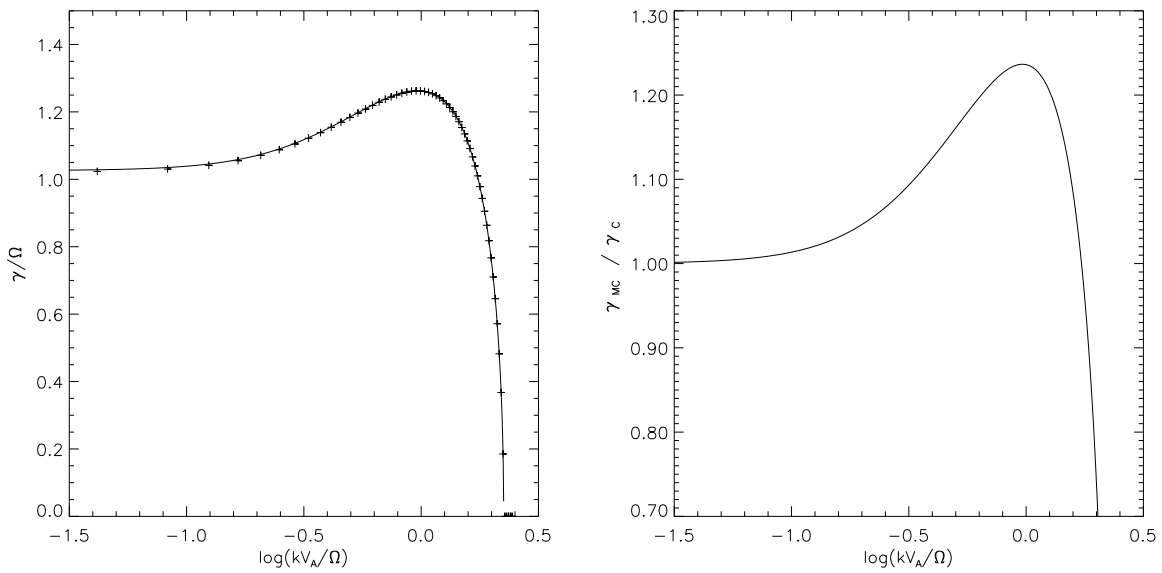


**Fig. 6.** Left panel: dimensionless growth rate  $\gamma/\Omega$  as a function of dimensionless wavenumber  $kv_A/\Omega$  for MHD equilibrium C (see table 1). The solid line corresponds with the solution from Narayan et al. (1994). The crosses correspond to the solution using the code LODDES. Right panel: ratio of the growth rate  $\gamma_{MC}$  with ( $\alpha_2 = 1.0$ ) and the growth rate  $\gamma_C$  without ( $\alpha_2 = 0.0$ ) an axial magnetic field component as a function of the dimensionless wavenumber  $kv_A/\Omega$ .

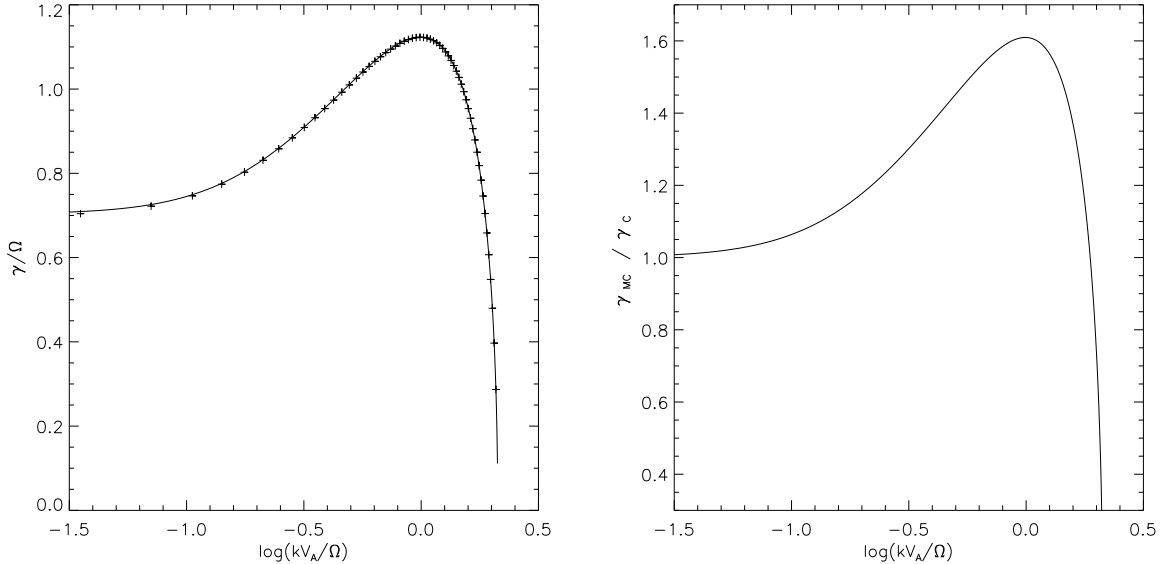


**Fig. 7.** Left panel: dimensionless growth rate  $\gamma/\Omega$  as a function of dimensionless wavenumber  $kv_A/\Omega$  for MHD equilibrium D (see table 1). The solid line corresponds with the solution from Narayan et al. (1994). The crosses correspond to the solution using the code LODDES. Right panel: ratio of the growth rate  $\gamma_{MC}$  with ( $\alpha_2 = 1.0$ ) and the growth rate  $\gamma_C$  without ( $\alpha_2 = 0.0$ ) an axial magnetic field component as a function of the dimensionless wavenumber  $kv_A/\Omega$ .

bers are significantly amplified by the magneto-rotational mechanism. Furthermore, model C shows that for axial wavenumbers  $\log(kv_A/\Omega) < -1.0$ , the contribution of the magneto-rotational mechanism has decreased to a few percent. This indicates that the unstable modes in this range of wavenumbers have a dominant convective nature. This conclusion on the long wavelength regime was also made by Narayan et al. (2002) in their analysis.

Finally, Figure 7 shows our results for model D, which has a corresponding value of the ratio  $N^2/\Omega^2 = 1.5$  (see Table 1). The left panel of Figure 7 shows the calculated growth rates (crosses) of this MHD equilibrium, in agreement with the solution (solid line) from Narayan et al. (2002). The right panel of Figure 7 shows the ratio of the growth rate of model D with axial magnetic field ( $\alpha_2 = 1.0$ ) with respect to model D without an ax-

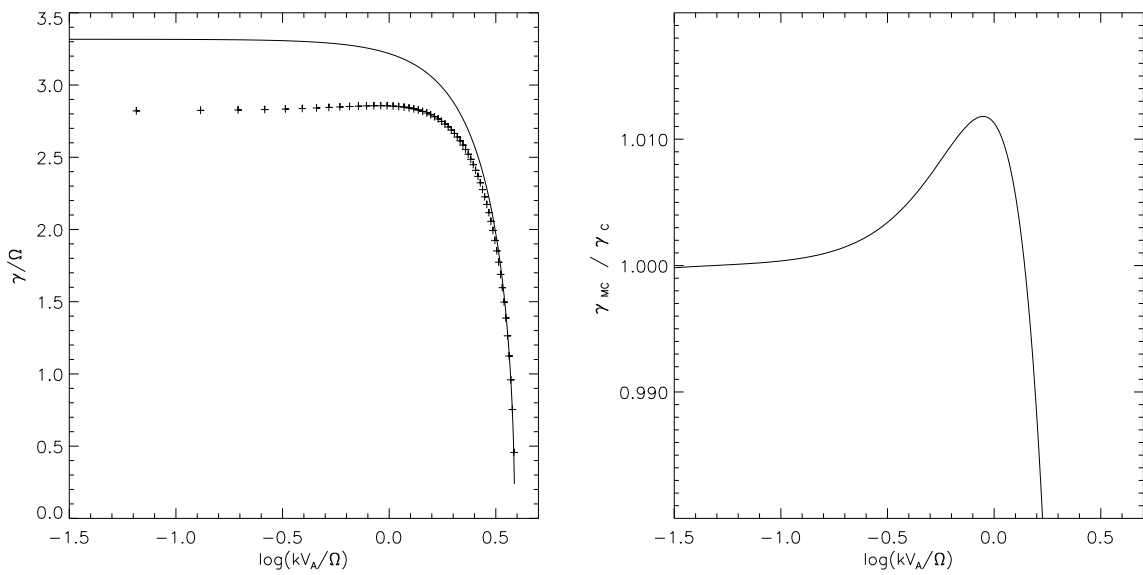


**Fig. 8.** Left panel: dimensionless growth rate  $\gamma/\Omega$  as a function of dimensionless wavenumber  $kv_A/\Omega$  for MHD equilibrium E (see table 1). The solid line corresponds with the solution from Narayan et al. (1994). The crosses correspond to the solution using the code LODES. Right panel: ratio of the growth rate  $\gamma_{MC}$  with ( $\alpha_2 = 1.0$ ) and the growth rate  $\gamma_C$  without ( $\alpha_2 = 0.0$ ) an axial magnetic field component as a function of the dimensionless wavenumber  $kv_A/\Omega$ .

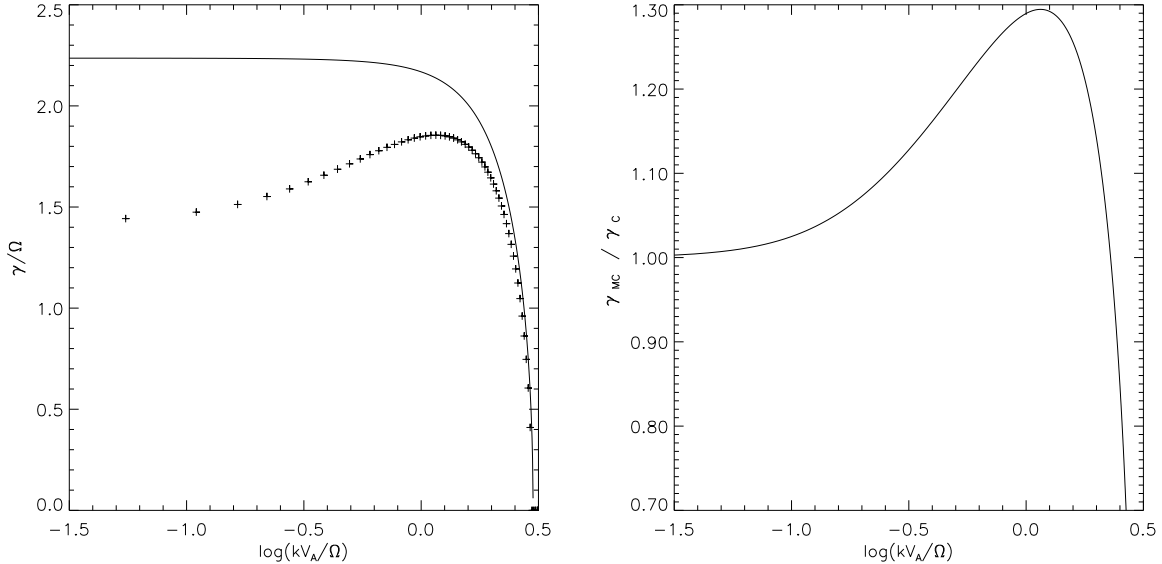


**Fig. 9.** Left panel: dimensionless growth rate  $\gamma/\Omega$  as a function of dimensionless wavenumber  $kv_A/\Omega$  for MHD equilibrium F (see table 1). The solid line corresponds with the solution from Narayan et al. (1994). The crosses correspond to the solution using the code LODES. Right panel: ratio of the growth rate  $\gamma_{MC}$  with ( $\alpha_2 = 1.0$ ) and the growth rate  $\gamma_C$  without ( $\alpha_2 = 0.0$ ) an axial magnetic field component as a function of the dimensionless wavenumber  $kv_A/\Omega$ .

ial magnetic field component ( $\alpha_2 = 0.0$ ). The contribution from the magneto-rotational mechanism is increasing up to 60 percent around values of the wavenumber where the growth rate has its maximum. For axial wavenumbers  $\log(kv_A/\Omega) < -1.0$ , the contribution of the magneto-rotational mechanism has a maximum of order 5 percent, which indicates their dominant convective nature.

The models C and D discussed above have the same ratio of  $N^2/\Omega^2$  as the models discussed by Narayan et al.(2002). Our conclusions confirm those by Narayan et al.(2002) for the unstable long-wavelength modes ( $kv_A \ll \Omega$ ) in these two models: they are clearly convective modes. However, the wavelength modes in these models with  $kv_A \sim \Omega$  are shown to be maximally amplified by the magneto-rotational mechanism: the amplification is in-

creasing as the ratio  $N^2/\Omega^2$  is decreasing. However, these modes seem to be determined by both the convective and the magneto-rotational mechanism. Finally, for modes with  $kv_A > \Omega$ , the amplification of the growth rate is shown to be decreasing, due to the restoring magnetic tension force.

### 4.3. From weakly magnetized disks to disks close to equipartition

In this subsection we investigate the influence of the magnetization on the nature of the instabilities in our considered MHD equilibria (models E & F, Table 1).

Figure 8 shows our results for model E. The considered MHD equilibrium has the same parameters as model A from the previous subsection, except this one is closer to equipartition ( $\beta = 20$ ). Due to the stronger magnetic field, this equilibrium has a lower value of the ratio  $N^2/\Omega^2$  (see Table 1). Our calculations (crosses) and the calculation from Narayan et al. (2002) (solid line) deviate from each other, since the equation used by Narayan et al. (2002) is not valid for this model. This is because the toroidal magnetic field strength can not be neglected anymore in the linear analysis, a component which was not taken into account in the equation used by Narayan et al. (2005). Contrary to the model A, this model shows a maximum value of the growth rate, close to the typical value of the magneto-rotational instability, i.e.  $\log(kv_A/\Omega) \approx 0.0$ . The right panel shows the ratio of the growth rate of model E with axial magnetic field ( $\alpha_2 = 1.0$ ) with respect to model E without an axial magnetic field component ( $\alpha_2 = 0.0$ ). There is a slight enhancement observed close to the maximum value of the growth rate: this indicates that the magneto-rotational mechanism starts to contribute to the growth rate of unstable modes in this region. Notice that the enhancement is still very weak, of order 1 percent (right panel Figure 8).

Finally, figure 9 shows our results for model F. In this MHD equilibrium the magnetization is close to equipartition ( $\beta = 10.0$ ), with a corresponding value  $N^2/\Omega^2 = 6.0$  (see Table 1). We notice that we do not consider a disk in exact equipartition (i.e.  $\beta = 1.0$ ), because this model would not allow for convective instabilities (i.e.  $N^2/\Omega^2 < 1$  as can be seen in Figure 3). The left panel of Figure 9 shows that the approximation from Narayan et al. (2002) (solid line) is no longer valid. Taking into account the toroidal magnetic field component, our calculations show a distinct maximum which occurs at the typical value  $\log(kv_A/\Omega) = 0.0$  for magneto-rotational instabilities. The right panel of figure 9 shows the ratio of the growth rate of model F with axial magnetic field ( $\alpha_2 = 1.0$ ) with respect to model F without an axial magnetic field component ( $\alpha_2 = 0.0$ ). It can be observed that in the region around the maximum of the growth rate, the contribution of the magneto-rotational mechanism is of order 30 percent. This increase indicates that the unstable modes in this range of wavenumbers are significantly amplified

by the magneto-rotational mechanism. However, for axial wavenumbers  $\log(kv_A/\Omega) < -1.0$ , the contribution of the magneto-rotational mechanism has decreased to a few percent. This indicates that the unstable modes in this range of wavenumbers have a dominant convective nature.

## 5. Conclusions

We calculated growth rates of instabilities for MHD equilibria of magnetized accretion disks. The disks models were taken in the cylindrical limit and included both toroidal and axial magnetic field components. Due to the presence of a toroidal magnetic field component, the unstable modes we find are strictly speaking *overstable* modes (see e.g. Blokland et al., 2005). The parameters of the model in our calculations were taken such that the axial wavenumber of the most unstable modes were larger than the inversed scale height  $H$ . Therefore the analysis can be used as an approximation for a stability analysis of the interior of an accretion disk. Our models considered both weakly magnetized disks, as well as disks which are close to equipartition. All calculations were performed with a restriction to axisymmetric perturbations ( $m = 0$ ).

Our most important results are summarised below:

- We have considered models of thick accretion disks, which are subject to convective magneto-rotational instabilities, and we quantified the contribution of the MRI mechanism of all the instabilities considered.
- Our calculations are diverging from the solutions from Narayan et al.(2002), when the disk models are becoming significantly magnetized. The deviations are contributed to the toroidal magnetic field component, which was neglected in the derivation of the equation for the growth rate used by Narayan et al.(2002).
- Our calculations show that the contribution from the magneto-rotational mechanism to the growth rate becomes significant as the disks get close to equipartition. The contribution peaks for modes near the maximum value of the growth rate.
- Our calculations for the growth rates agree with the calculations from Narayan et al. (2002) for weakly magnetized accretion disk models, even though we include dominant toroidal field components.
- Our calculations show that the contribution from the magneto-rotational mechanism to the growth rate becomes significant as the scale-height  $H$  is decreased. This contribution peaks for modes near the maximum value of the growth rate.
- All our calculations show that the contribution from the magneto-rotational mechanism to the growth rate becomes negligible for unstable modes with  $\log(kv_A/\Omega) < -1.0$ , which are safely interpreted as purely convective modes in all cases.

*Acknowledgements.* JWB and RK carried out this work within the framework of the European Fusion Programme, and it is supported by the European Communities under the contract of Association between EURATOM/FOM. Views and

opinions expressed herein do not necessarily reflect those of the European Commission. EvdS did this research in the FOM projectruimte on 'Magnetoseismology of accretion disks', a collaborative project between R. Keppens (FOM Institute Rijnhuizen, Nieuwegein) and N. Langer (Astronomical Institute Utrecht). This work is part of the research programme of the 'Stichting voor Fundamenteel Onderzoek der Materie (FOM)', which is financially supported by the 'Nederlandse Organisatie voor Wetenschappelijk Onderzoek (NWO)'.

## References

- Baganoff, F. K., Bautz, M. W., Brandt, W. N., Chartas, G., Feigelson, E. D., Garmire, G. P., Maeda, Y., Morris, M., Ricker, G. R., Townsley, L. K., Walter, F. 2001, *Nature*, 413, 45
- Balbus, S. A., Hawley, F. H. 1991, *ApJ*, 376, 214
- Balbus, S. A., Hawley, F. H. 2002, *ApJ*, 573, 749
- Blokland, J. W. S., van der Swaluw, E., Keppens, R., Goedbloed, J. P. 2005, *A&A*, *in press*
- Christodoulou, D. M., Contopoulos, J., Kazanas, D. 2003, *ApJ*, 586, 372
- Di Matteo, T., Allen, S. W., Fabian, A. C., Wilson, A. S., Young, A. J. 2003, *Ap*, 582, 133
- Hawley, J. F. 2001, *ApJ*, 554, 534
- Keppens, R., Casse, F., Goedbloed, J. P. 2002, *ApJ*, 569, L121
- Narayan, R., Yi, I. 1994, *ApJ*, 428, L13
- Narayan, R., Quataert, I. V., Igumenshchev, I. V., Abramowicz, M. A. 2002, *ApJ*, 577, 295
- Press, W. H., Teukolsky, S. A., Vetterling, W. T., Flannery, B. P. 1988, *Numerical Recipes* (New York: Cambridge Univ. Press)
- Shakura, N. I., Sunyaev, R. A. 1973, *A&A*, 24, 337
- Tassoul, J. L. 1987, *Theory of Rotating Stars* (Princeton University Press)
- Wang, C., Blokland, J. W. S., Keppens, R., Goedbloed, J. P. 2004, *J. Plasma Phys.* 70(6), 651-669.